Built on LDRD Laboratory Directed Research and Development

SAND20XX-XXXXR
LDRD PROJECT NUMBER: 189267
LDRD PROJECT TITLE: Material Testing for Shear-Dominated Ductile Failure
PROJECT TEAM MEMBERS: Edmundo Corona (PI), Sharlotte Kramer and Brian Lester

ABSTRACT:

An initial foray into the design of specimens that can be used to provide data about the quasi-static ductile failure of metals when subjected to shear-dominated (low triaxiality) states of stress was undertaken. Four specimen geometries made from two materials with different ductility (Al 7075, lower ductility and steel A286, higher ductility) were considered as candidates. Based on results from analysis and experimentation, it seems that two show promise for further consideration. Whereas preliminary results indicate that the Johnson-Cook model fit the failure data for Al 7075 well, it did not fit the data for steel A286. Further work is needed to consolidate the results and evaluate other failure models that may fit the steel data better, as well as to extend the results of this work to the dynamic loading regime.

INTRODUCTION:

Many mechanics problems of interest at Sandia involve the response and failure of components and structures under severe environments. Typically, the structures and loadings of interest are quite complex, and analysts must resort to computational models in order to draw conclusions that can be used in a variety of decision-making scenarios related to Sandia's national security mission. The representation of the behavior and failure of materials plays a very important role on the fidelity of the structural computational models. Many material models are available, and the choices that an analyst makes depend on the type of material used in the applications, the ease of calibration and cost of the model, and the particulars of the geometry and loading of interest. This work concentrates on metallic alloys that behave as elastic-plastic solids and fail in a ductile manner after significant plastic deformation.

Essentially all useful material models used in practice are phenomenological, meaning that they are formulated to attempt to reproduce observations of material behavior as measured in the laboratory at a scale similar to that of the applications. Therefore, the constitutive and/or failure models must be calibrated according to data obtained from material tests. This makes material testing an essential part of computational predictions, and the quality of such predictions is strongly tied to the test data through several aspects of the test and calibration process. First, it is important that the material tests explore stress paths that are representative of those that arise in the structural applications of interest. This can be accomplished through careful design of the material test specimens and loading conditions. Second, data related to both the load and deformation of the specimens must be carefully collected and analyzed. Appropriate data acquisition that captures relevant measurements is very important. Third, the model calibration process must be closely tied to the material tests and must consider the interpretation the data

acquired with respect to both the problem being considered and the parameters of the numerical model of the application. Therefore, the calibration process often includes numerical simulations of the material tests in order to extract data that can be used in the model of the application. This is particularly true when the material specimen geometry is somewhat complex and/or when the specimens undergo large, non-homogeneous deformations.

This work concentrated on the design of specimens where the state of stress was dominated by shear and where the main objective was obtaining failure data. Whereas testing under tensile-dominated stresses can be achieved using traditional tests such as uniaxial tension and notched tension, data for shear-dominated loading is more difficult to obtain. The principal reason is that shear testing is significantly more difficult than tensile testing and no standards exist. These difficulties extend to specimen design, data acquisition and calibration procedures. The objective of this project was to explore test configurations and specimen geometries that can be designed to induce shear-dominated failure in the material. This project utilized combined numerical and experimental approaches to achieve its goals. The numerical approach was used during the design phase of the more complex test geometries. Following the design and manufacture, the specimens were tested to failure in the laboratory. Subsequent comparison between the results from the tests and the analysis provided the means to assess the usefulness of the specimen and test design to induce material failure under shear-dominated states of stress.

DETAILED DESCRIPTION OF METHOD:

Four specimen geometries and their associated quasi-static loading conditions were considered in this project with the objective of evaluating their suitability to generate ductile failure data when the state of stress was shear-dominated. Two materials were considered for each geometry: Al 7075-T651 and steel A286. From our perspective, the main difference between the two materials was their ductility. The aluminum alloy was significantly less ductile than the steel alloy. The intention was to see whether the same or different failure models would be required to fit failure data for different materials, especially those with significantly different ductility.

The method used to carry out the project combined analysis and experimentation. Analysis played two roles: first to aid with the design of the specimen geometries and second to help calibrate and evaluate the ductile failure model used in the study. The material failure model considered was that by proposed by Johnson and Cook [1] while an elastic-plastic model with isotropic hardening was used to model the stress-strain behavior of the material. Since the tests were quasi-static, the plastic strain to failure in the model is a function of just the stress triaxiality and the loading history. Stress triaxiality is defined as the ratio of the mean (hydrostatic) stress to the von Mises stress in the material. Generally speaking, states of stress with triaxiality of 0.3 or larger are tensile-dominated, whereas those with triaxiality around 0 are shear-dominated. This project concentrates on evaluating specimens with respect to failure (or fracture) that starts in regions with near zero triaxiality.

Using analysis models to design the specimens introduces unavoidable ambiguity because a material failure model needs to be part of the analysis. The specimen design has to be carried out assuming that the predictions of the material failure model are correct, hence the importance of experimentation in this project to evaluate the failure predictions. It is only by direct comparison between the results of analysis and experimentation that one can tell how appropriate the material failure model was at the design stage. The interaction between analysis and experiment is therefore an essential part of research in the area of ductile failure.

One final note before introducing the specimen geometries considered: In order to efficiently address the objectives of this project in the relatively short time available to conduct the work, it was important to combine results from previous work with those obtained during the course of the funding period. For example, two of of the specimens had previously been designed and previous test results were already available for one. This project supported the analysis of the data in the latter case.

Figure 1 shows the four specimen geometries while Fig. 2 shows schematics of the loading applied in each case. The four cases considered were:

1. **Hat specimen under compression**, shown in Figs. 1 and 2 (a). This specimen was originally designed by Brad Boyce and Brad Salzbrenner of Org. 1851 for the 2013 Sandia Fracture Challenge. The overall width, height and thickness of the specimen are 1.63, 1.25 and 0.40 inches, respectively. Under compression, the deformation of the specimen is concentrated in the two regions above the top corners of the hole. This specimen received further attention in a subsequent experimental study [2], where the test data used here were obtained.
2. **EDM notch specimen under direct shear**, shown in Figs. 1 and 2 (b). This specimen is similar to those used as part of previous studies to study the response and failure of laser welds [3]. The specimen consists of a bar of rectangular cross-section, 0.125 by 0.25 inch on each side and with length of 4 inches. It contains an EDM notch at the center 0.062 inches wide over one-half of the bar depth. The specimen is loaded directly in shear using the test set up shown in Fig. 4 that will be described in more detail in the next section. Samples with this geometry had been previously manufactured with the intent of using them to investigate the ductile failure of the materials considered here under shear-dominated loading.
3. **Butterfly specimen under direct shear**, shown in Figs. 1 and 2 (c). The butterfly specimen was proposed in [4] with the intention of studying ductile failure under shear-dominated conditions. In our case, it consists of a bar of rectangular cross-section with a one inch height and 0.25 inch thickness. The length of the bar is 4 inches. A region of the bar in a shape resembling a butterfly, narrowest at the center of the height and wider towards the edges is machined to a thickness of 0.050 inches. The design idea is that, under direct shear loading, the shear strain at the narrowest section will be highest thus causing failure to not be influenced by free-edge effects. The dimensions of the butterfly

region, however, must be chosen carefully to achieve the desired outcome. After designing the proper geometry, several specimens were machined and tested.

4. **Smiley specimen under tension**, shown in Figs. 1 and 2 (d). This specimen was proposed in [5] as a way to subject the material to shear-dominated loading using a conventional uniaxial tension machine. By applying tension, the material in the regions that join the top part of the specimen to the bottom part is subjected to shear loading. According to [5], the shape of these regions need to be optimized in order to generate failure with near-zero triaxiality. After several design tries, we could not develop a good geometry that gave the desired results. Therefore, consideration of this specimen was discontinued without manufacturing any.

In summary, out of the four specimen geometries considered two had already been designed, leaving two to be designed. One geometry was discarded prior to testing, leaving three specimen types that were tested and pursued further. The results obtained will be presented in the next section, after describing the test set-ups used.

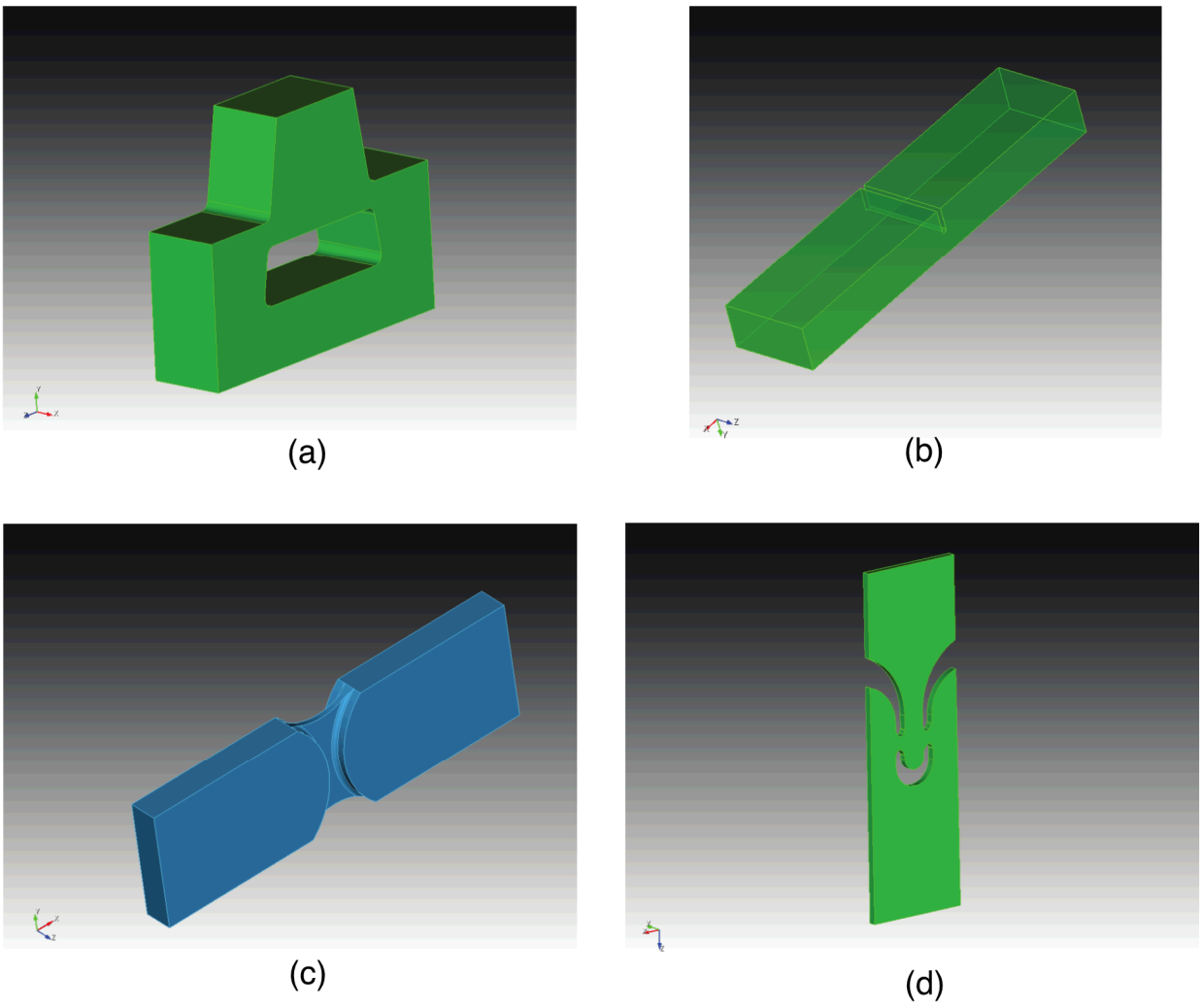

Figure 1: Four test geometries considered. (a) Hat, (b) EDM-notch, (c) butterfly and (d) Smiley.

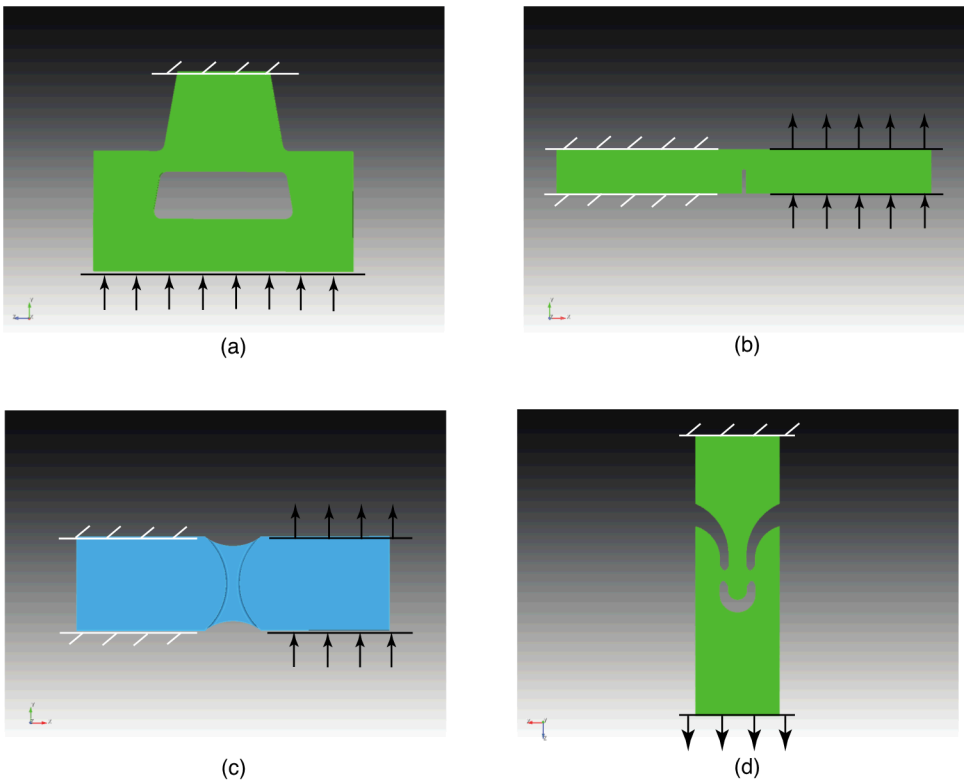

Figure 2: Applied loading to the four test geometries. (a) Hat specimen under compression, (b) EDM-notch specimen under direct shear, (c) butterfly specimen under direct shear and (d) smiley specimen under tension.

Figure 3 shows the test set-up used to load the hat specimens. The compression platens were attached directly to the load cell and the actuator of the testing machine. The platens were circular and 4 inches in diameter. They were machined from A2 tool steel and hardened to Rockwell C 45 with a #8 mirror surface finish. They were installed such that the flat surfaces were parallel within 0.001 inches across the diameter in any direction. The load was measured by a 22-kip calibrated load cell while the relative distance between the platens was measured via four linearly variable differential transformers (LVDTs) to allow detecting tilting of the platens during loading. Platen tilting was negligible if the specimen was carefully placed at the center of the platens. The specimens were loaded quasi-statically in displacement control at a rates of either 0.001 or 0.0001 in/s. No significant differences were seen between the responses measured for the two rates. In addition, one surface of the specimen was painted with a speckle pattern in order to make surface deformation measurements using digital image correlation (DIC). Correlated Solutions VIC-3D was used to analyze the DIC data. The subset size in the DIC measurements was 85x85 pixels with a step size of 10 pixels, and the length of the virtual strain gage was approximately 0.013 in. The frame rate of the stereo cameras used to image the specimens was 2.5 kHz or 0.5Hz, depending on the speed of loading.

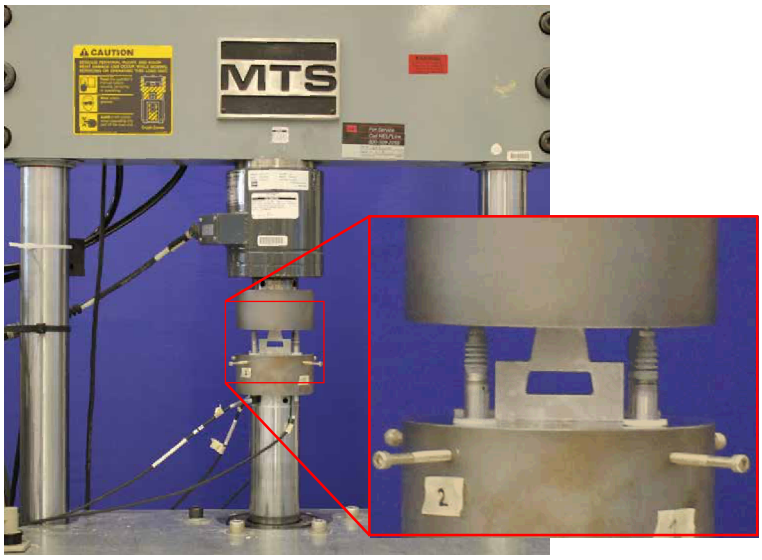

Figure 3: Photograph showing the hat specimen between the compression plates, which were mounted in a standard 22 kip test frame.

Both the EDM-notched and butterfly specimens were tested by applying direct shear in a custom test fixture in the Structural Mechanics Laboratory. The fixture is composed of two clevises with grip inserts that can be adjusted to accommodate different specimen thicknesses and desired grip gaps (horizontal distance between the two grips). Figure 4 shows two views of the fixture: Fig. 4(a) shows the fixture installed with the axial LVDTs, and Fig. 4(b) shows the full setup with imaging cameras. The upper clevis is attached to a vertical servo-hydraulic actuator, and is therefore the moving side. The lower clevis, the stationary side, is attached to a rigid bar with two equally spaced load cells that are attached to the load frame table; these two load cells can be summed to measure the total load or can be used to measure the moment across the specimen. The fixture can be configured into five loading setups ranging between pure tension to Mode-II shear, with three intermediate mixed-mode loading setups. For this study, the fixture was in the Mode-II setup as shown in Fig. 4**.** The setup included two sets of cameras: the single camera setup in the foreground Fig. 4(b) viewed a bare metal side of the specimens and the two-camera setup on the opposite side viewed a painted speckled pattern for DIC measurements of full-field surface displacement and strain. The vertical actuator moved at a quasi-static displacement rate of 0.0001 in/s, and the camera acquisition rate was 1-4 Hz depending on the specimen. Figure 5 shows the DIC field of view for the EDM-notched and butterfly specimens. The grip gap for the EDM-notched specimens and for the butterfly specimens were 0.125 inch and 0.712 inch, respectively. Both the specimens and the grips were speckled using an airbrush so that the local motion of the specimens and the grips could be measured. Correlated Solutions VIC-Snap program was used to acquire in the images. Correlated Solutions VIC-3D was used to analyze the DIC data. For the EDM-notched specimens, the DIC subset size was 41 pixels, the step size was 5 pixels, and the virtual strain gage size was 81 x 81 pixels (0.0137 x 0.0137 in). For the

butterfly specimens, the DIC subset size was 37 pixels, the step size was 5 pixels, and the virtual strain gage size was 77 x 77 pixels (0.0314 x 0.0314 in).

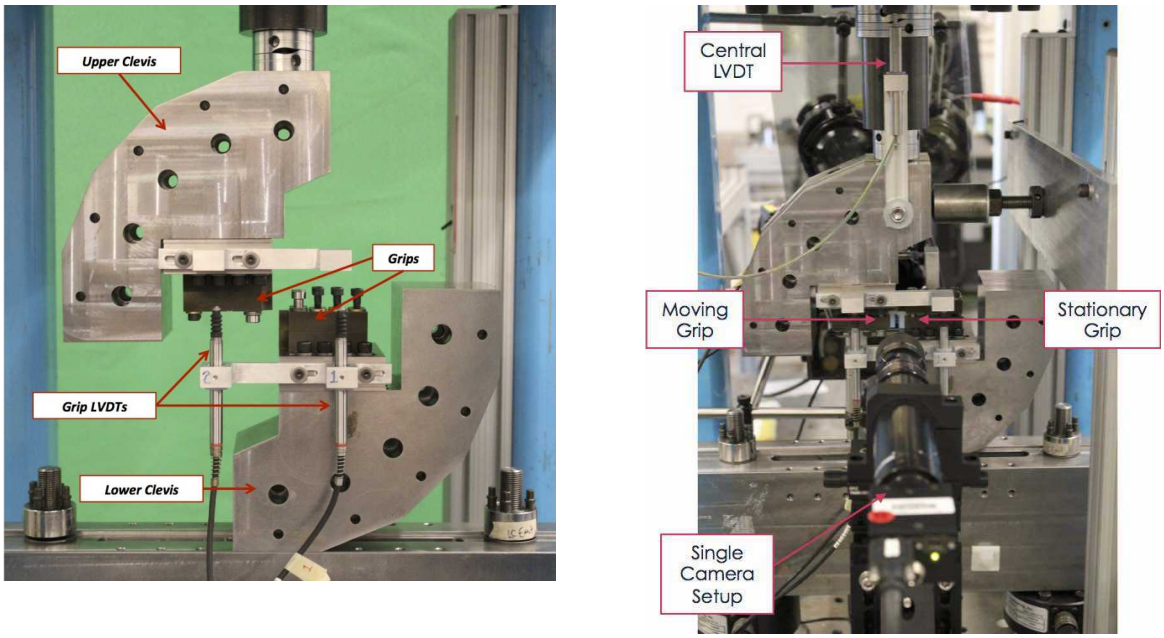

(a) (b)

Figure 4: Custom test fixture for direct shear application. (a) Bare fixture installed and (b) fixture with installed specimen and camera setups.

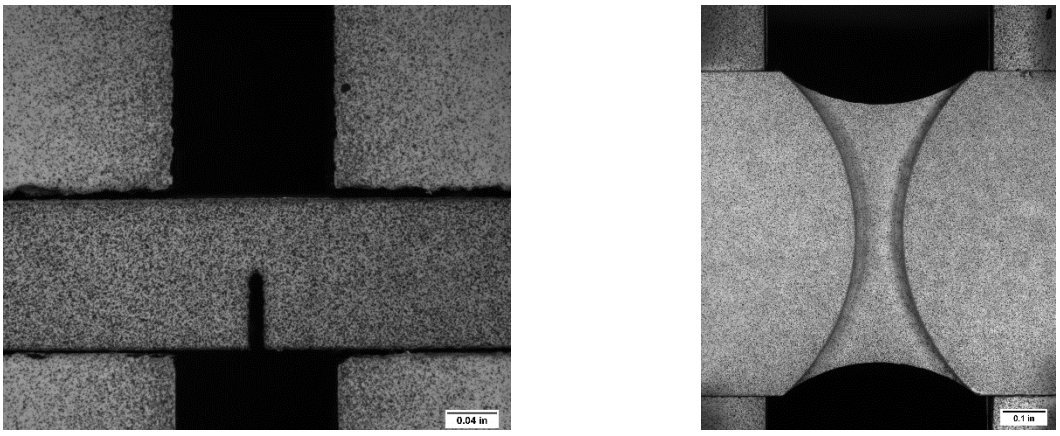

(a) (b)

Figure 5: (a) DIC field of view for the EDM-notched specimens and (b) DIC field of view of the butterfly specimens. The photographs show the painted speckle pattern on the surface of the specimens and the grips.

RESULTS:

The design calculations were conducted principally using the properties of the Al 7075 alloy found in [6], and the relevant results will be shown for each of the four specimen geometries. Some calculations were also conducted for the steel A286 specimens in order to advise the laboratory regarding the load levels that could be expected during the experiments. In general, the load levels predicted by the analysis were in the vicinity of those achieved in the laboratory.

Hat specimen

Design calculations were not conducted in this case because the specimens had already been manufactured and tested prior to the beginning of this project. We will, however, use analysis results to illustrate what the desirable characteristics of the specimen design are. Figure 6(a) shows the Johnson-Cook damage in the region of interest in an Al 7075 specimen just prior to failure. A value of zero, shown in blue, represents no damage whereas a value of 1, shown in red, represents initiation of failure of the material. Figure 6(b) shows the stress triaxiality, also just prior to failure. Recall that if the state of stress is shear dominated the triaxiality should be about zero, which is shown in green. A desirable specimen design is one that produces the largest damage in an area near zero triaxiality. Comparison of the results in both figures show that the hat specimen meets this requirement.

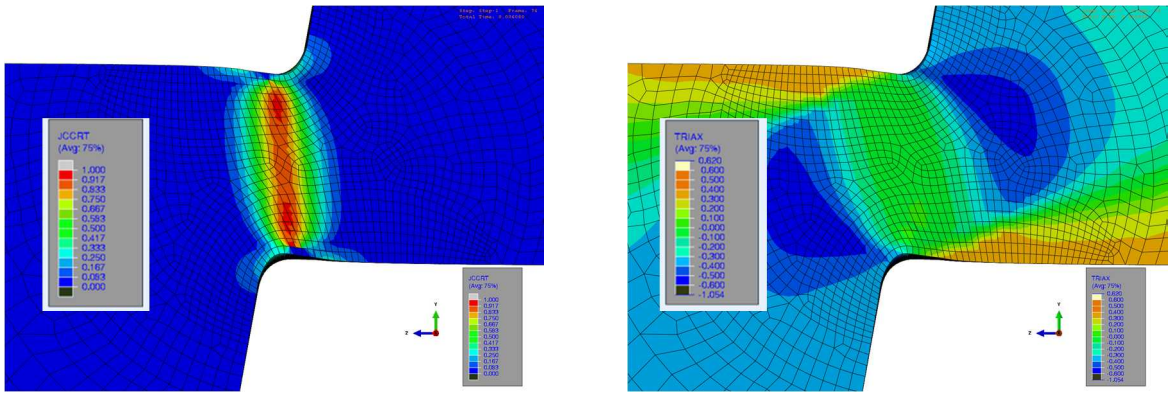

(a) (b)

Figure 6: (a) Contours of Johnson-Cook damage on the surface of the specimen and (b) Contours of stress triaxiality for the same surface.

Figure 7 shows the test results for an Al 7075 hat specimen. Figure 7(a) shows the measured load-deflection response while Fig. 7(b) shows contours of shear strain measured using DIC at point 3 in Fig. 7(a). The failure of the specimen occurred suddenly just after point 3. Note that the shear strain is highly localized in the specimen and that it is highest in the regions where the analysis predicted maximum damage. The analysis results showed the same concentration of shear strain.

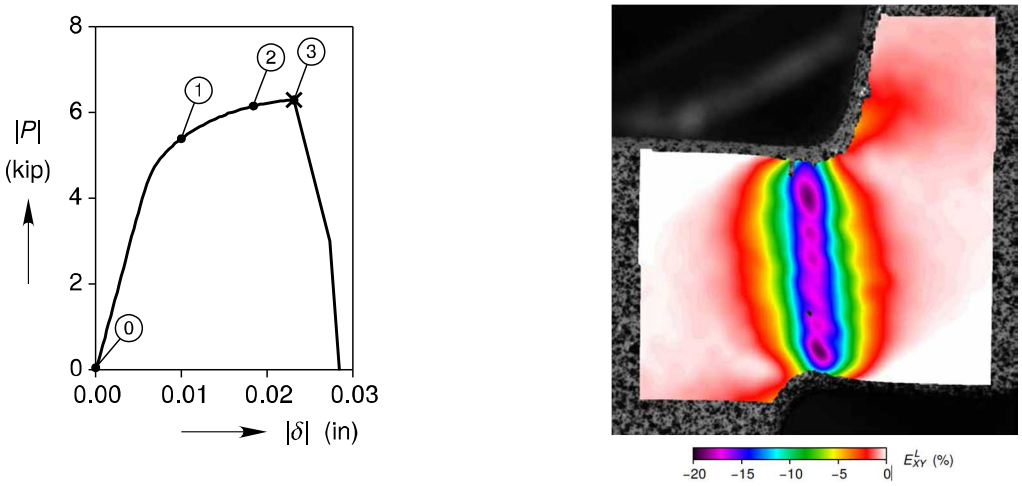

(a) (b)

Figure 7: Test results for an Al 7075 hat specimen. (a) Load-deflection response and (b) Contours of logarithmic shear strain on the surface of the specimen at point 3, just prior to failure.

Figures 8(a) and (b) show similar results for steel A286. Compared to the aluminum specimen, the steel specimen achieved much higher loads and deformations. In particular, the load-deflection response showed a limit load, followed by gradual decrease in the load, something that was not observed in the aluminum specimens. Further experimental work [2] showed that the load drop was due to the growth of cracks in the specimen, and that material failure had already started by the point where the maximum load occurred.

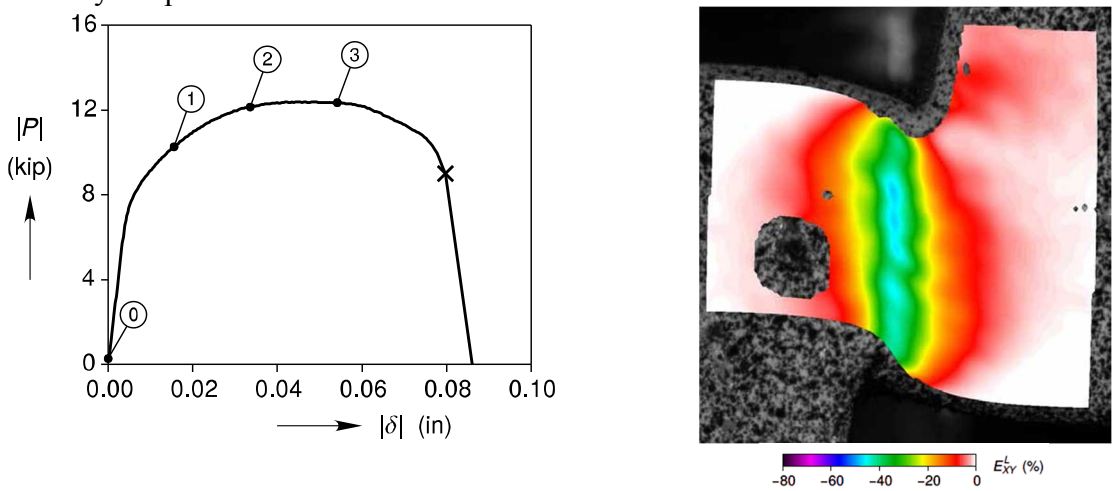

(a) (b)

Figure 8: Test results for a steel A286 hat specimen. (a) Load-deflection response and (b) Contours of logarithmic shear strain on the surface of the specimen at point 3, near the

maximum load.

The results obtained with the hat specimen were analyzed in more detail than the rest of the geometries considered. Examples of the results for Al 7075 are shown in Fig. 9. Comparisons of the measured and predicted load-deflection responses show that the analysis overestimated the load in the specimen by a small amount. Further test and analysis demonstrated that the material exhibited anisotropic yielding and that accounting for it through a simple calibration of the Hill anisotropic yield model improved the comparison. Regarding failure, the failure model was only implemented in conjunction with the original isotropic constitutive model and the predicted displacement at failure agreed reasonably well with the measured value. Figure 9(b) shows that the fit of the Johnson-Cook failure model approaches the failure data (filled symbols in the figure) reasonably well. The failure data include points from notched specimens under tension, smooth uniaxial tension test specimen and the newly generated point for the hat specimen.

Similar work performed using the steel A286 material, however, showed that the Johnson-Cook model did not fit that material well. Using a calibration based on notched specimens under tension predicted that the hat specimen would be much tougher in shear than was observed experimentally.

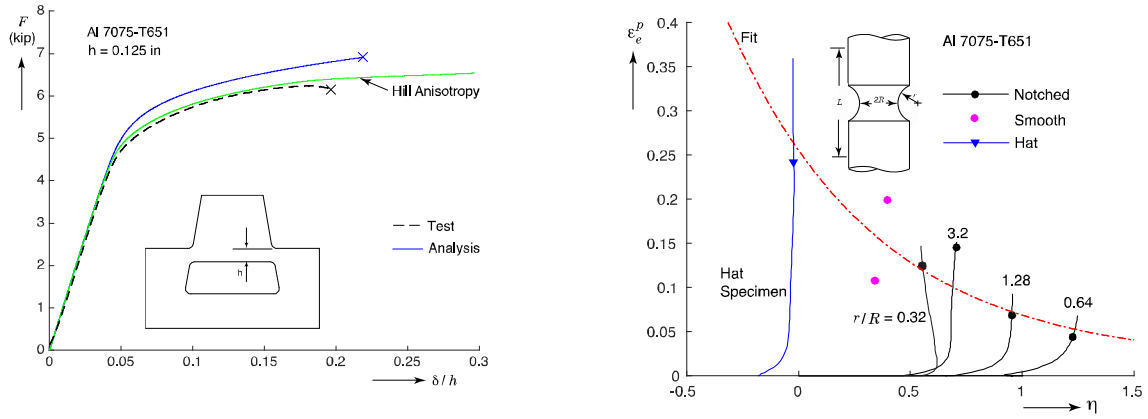

(a) (b)

Figure 9: Calibration results for the hat specimens. (a) Comparisons of measured and predicted load-deflection curves and (b) calibration failure points in plastic strain vs. triaxiality plot.

EDM-Notch Specimen

The EDM-notch specimens had been manufactured prior to the start of the current project. Testing, however, was conducted with the support of this project. Results for damage and triaxialty distributions obtained using the properties of Al 7075 are shown in Figs. 10(a) and (b) respectively. Note that the shape of the originally semi-circular root of the notch evolved so that the radius of curvature increased on the left side of the notch but decreased on the right. The

region of highest damage occurred in the region where the radius of curvature increased, but this also corresponds to a region with relatively large triaxiality, therefore indicating that failure is likely to be tensile dominated. Based on these results, this specimen geometry does not appear to be favorable for obtaining shear-dominated failure data.

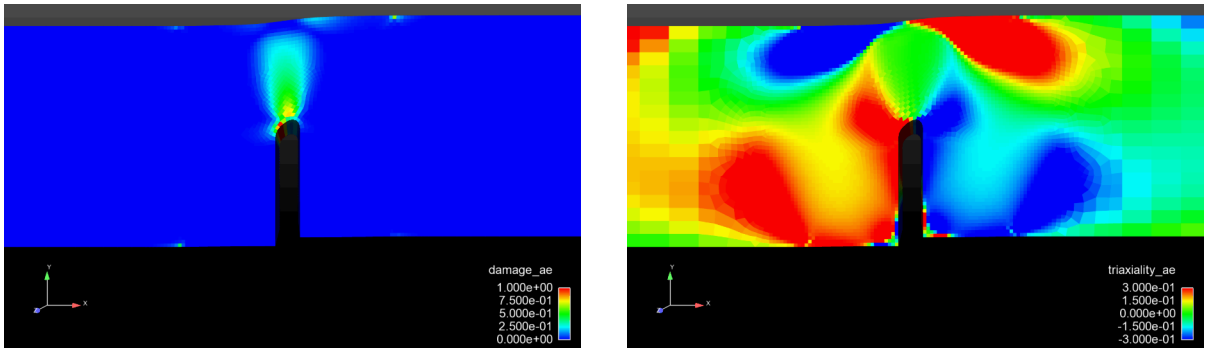

(a) (b)

Figure 10: Results of analysis for the EDM-notch specimen and Al 7075. (a) Contours of Johnson-Cook damage and (b) contours of stress triaxiality.

Specimens made of Al 7075 and steel A286 were tested in the laboratory and the load- deflection curves are shown in Fig. 11. As it was the case with the hat specimen, the steel specimen exhibited higher loads and displacement to failure than the aluminum one. Figure 12(a) shows a photograph of an aluminum specimen just prior to failure, at the point highlighted in Fig. 11. Contours of shear strain have been superimposed on the image, showing high values just above the notch. The specimen configuration after failure is shown in Fig. 12(b). The figure suggests that fracture occurred on the left side of the notch, as expected from the analysis. Confirmation can be carried out with more detailed imaging of the broken specimen. Figures 13(a) and (b) show similar images for the steel A286 specimen. Note that due to the much larger deflections, the deformation of the notch root is much more pronounced in this case. More surprisingly, Fig. 13(a) shows an indication of a crack on the region where the radius of curvature decreased, and Fig. 13(b) shows that the specimen was broken by a crack that intersected the right part of the notch. This contrasts with the failure of the aluminum specimen. This discrepancy is likely due to the interaction between the failure characteristics of the material and the much larger deformations attained in this case.

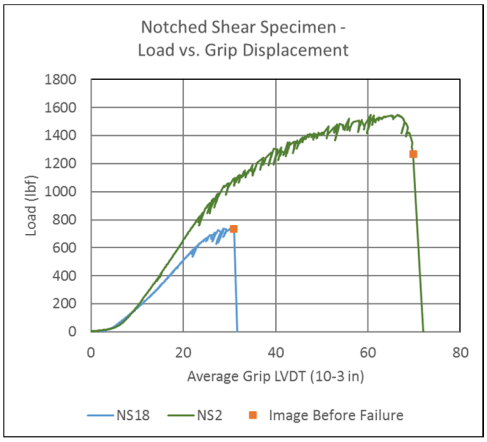

Figure 11: Measured load-deflection responses for an Al 7075 (NS18) and a steel A286 specimen (NS2).

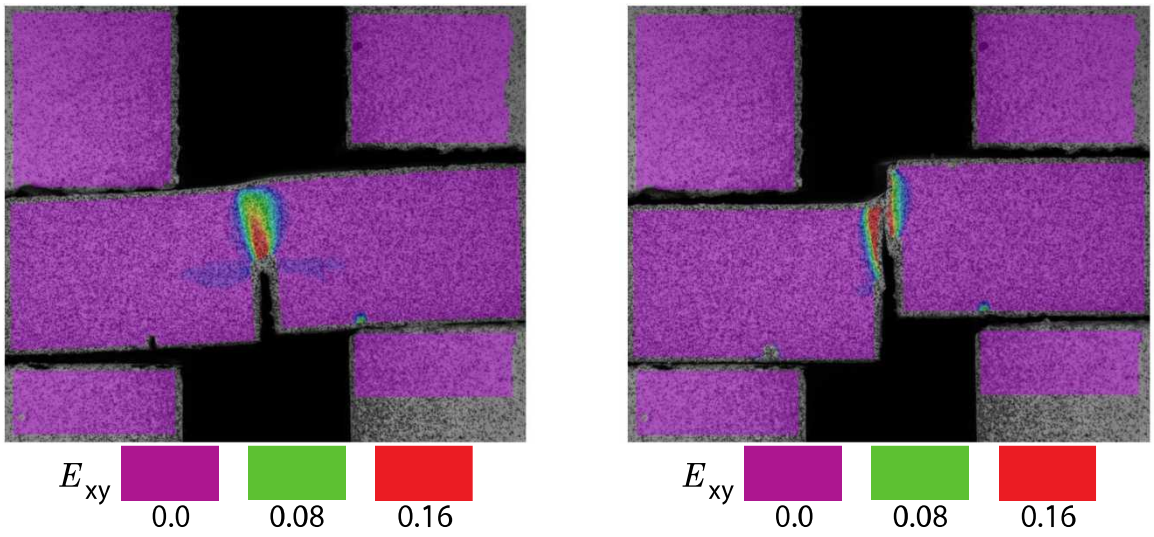

Figure 12: Al 7075 EDM-notch specimen configurations showing contours of shear strain. (a) Just prior to failure and (b) just after failure.

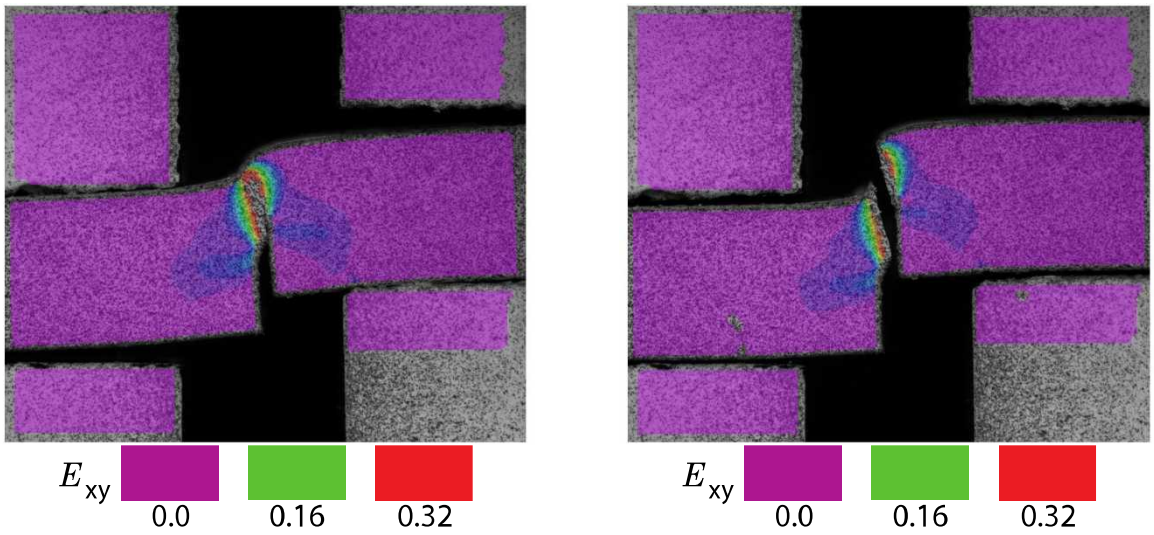

(a) (b)

Figure 13: Steel A286 EDM-notch specimen configurations showing contours of shear strain. (a) Just prior to failure and (b) just after failure.

Butterfly Specimen

The butterfly specimen was designed, manufactured and tested within the scope of the present project. The objective of this specimen is to have shear-dominated failure start away from the edges of the specimen. The key to achieve this objective was making the width of the test section at the top and bottom be at least 4 times the width at the center. This is to prevent the maximum value of Johnson-Cook damage from occurring at the regions with positive triaxiality at the top and bottom edges. Figure 14 shows the analysis results for this geometry. Note that the regions with maximum damage, shown in Fig. 14(a) occur well within the region where the triaxiality is near zero as seen in Fig. 14(b). Based on the analysis results, this specimen design is also promising to collect failure data under shear-dominated conditions.

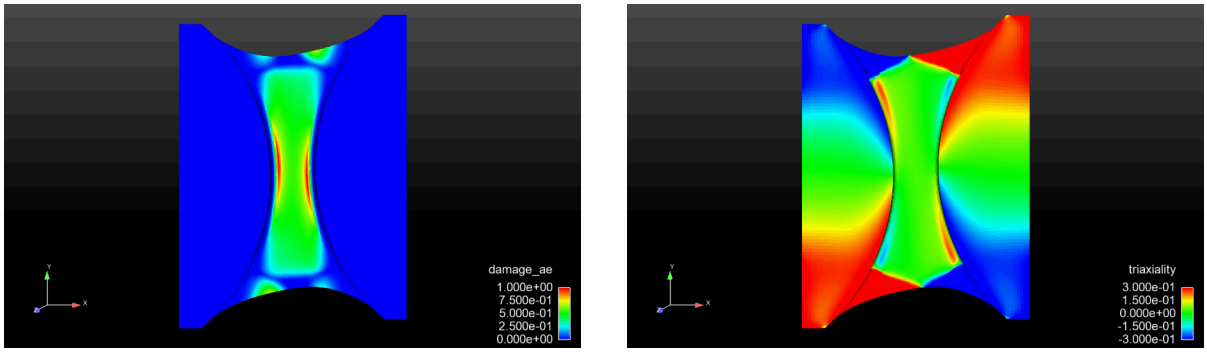

(a) (b)

Figure 14: Results of analysis for the butterfly specimen and Al 7075. (a) Contours of Johnson-Cook damage and (b) contours of stress triaxiality.

Figure 15 shows the load-deflection responses measured for this geometry. The comparison between the results obtained with the aluminum and steel alloys is similar to those obtained previously with one interesting difference: the steel results do not show a load maximum prior to failure.

Figures 16(a) and (b) show photographs of an aluminum test specimen just prior and after failure, respectively, with contours of shear strain superimposed. Note that the maximum shear strains occurred in the region where the analysis predicted the maximum damage. Looking at the failed specimen, the crack passed through the region where the shear strain was maximum. Whereas this observation alone does not guarantee that failure occurred first at those locations, it is nonetheless an encouraging sign. Figures 17(a) and (b) show similar results for a steel A286 specimen, except for the magnitude of the deformation prior to failure.

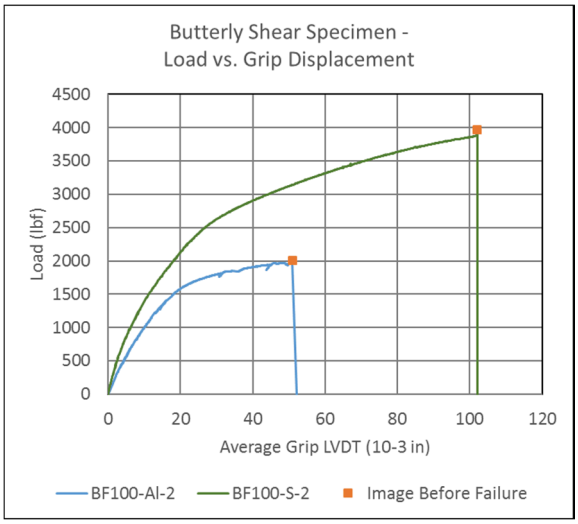

Figure 15: : Measured load-deflection responses for an Al 7075 (BF100-Al-2) butterfly and a steel A286 butterfly specimen (BF100-S-2).

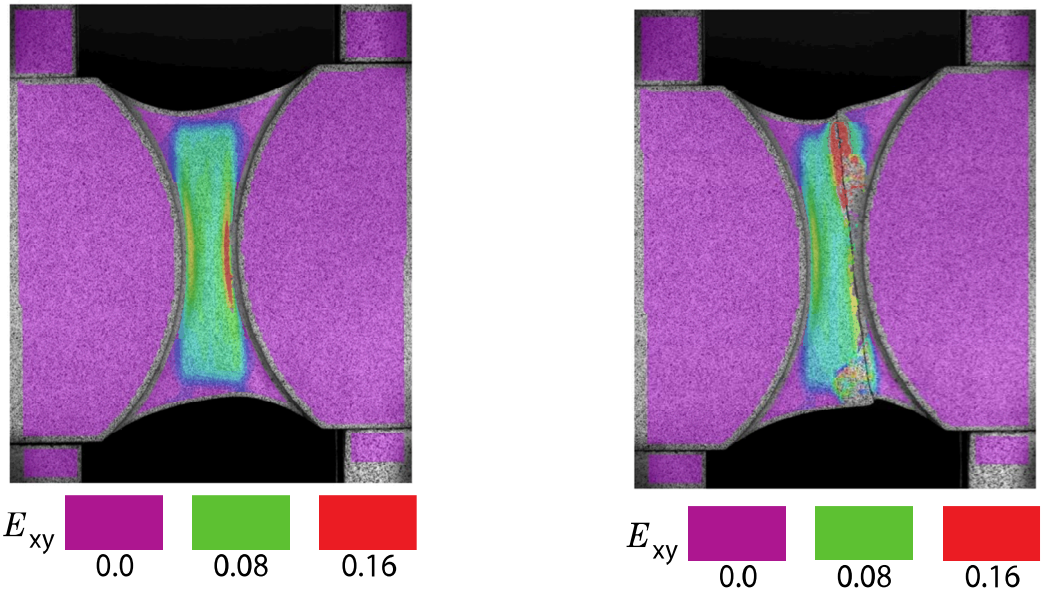

(a) (b)

Figure 16: Al 7075 butterfly specimen configurations showing contours of shear strain. (a) Just prior to failure and (b) just after failure.

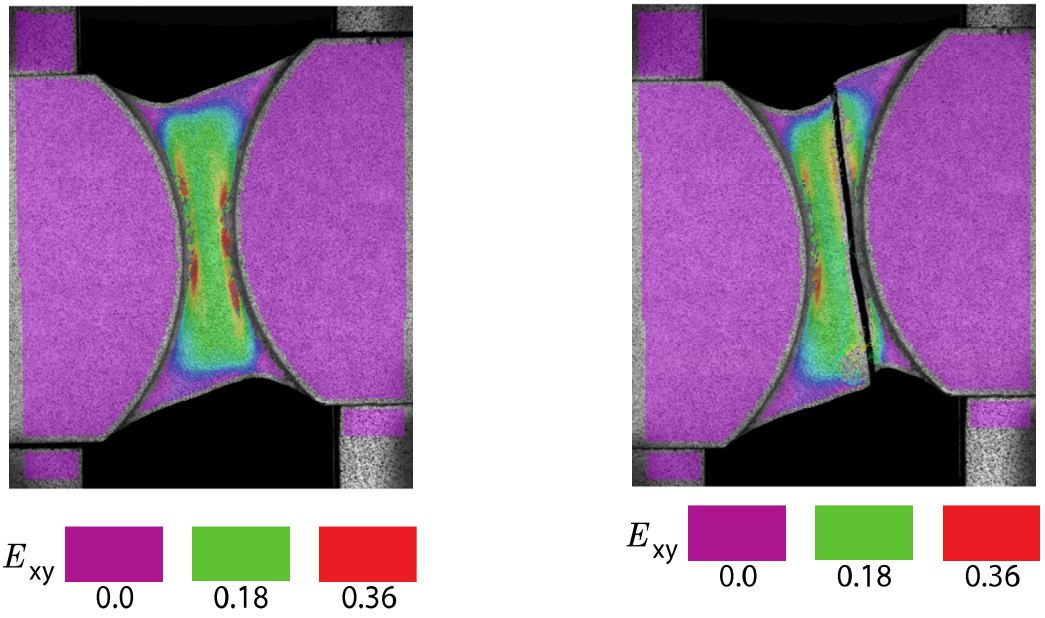

(a) (b)

Figure 17: Steel A286 butterfly specimen configurations showing contours of shear strain. (a) Just prior to failure and (b) just after failure.

Smiley Specimen

The last specimen considered was the smiley specimen, and the analysis results for Johnson-Cook damage and triaxiality are shown in Figs 18(a) and (b) respectively. The regions of high shear occurred between the roots of the notches, where the damage also concentrated. The numerical simulations for Al 7075, however, showed that the maximum damage occurred at the root of the notches where the triaxiality was positive. Note that the notch roots depicted were not initially circular because reference [5] pointed out that, according to the failure criterion used there, more optimal root notch geometries could be achieved to move the location of maximum damage away from the edges. Several attempts at different notch geometries including initially circular configurations and the design recommended in [5] were tried, but the maximum Johnson-Cook damage always occurred in regions of high triaxiality. It should be noted that different constitutive and failure models from the ones used here were employed in [5] to optimize the notch geometry. Even with the optimized configuration, the experimental results in [5] could not conclusively resolve whether or not failure initialized away or at the notch surface. Based on the analysis results obtained here, this geometry was considered unfavorable for the objectives of the project and was not pursued further.

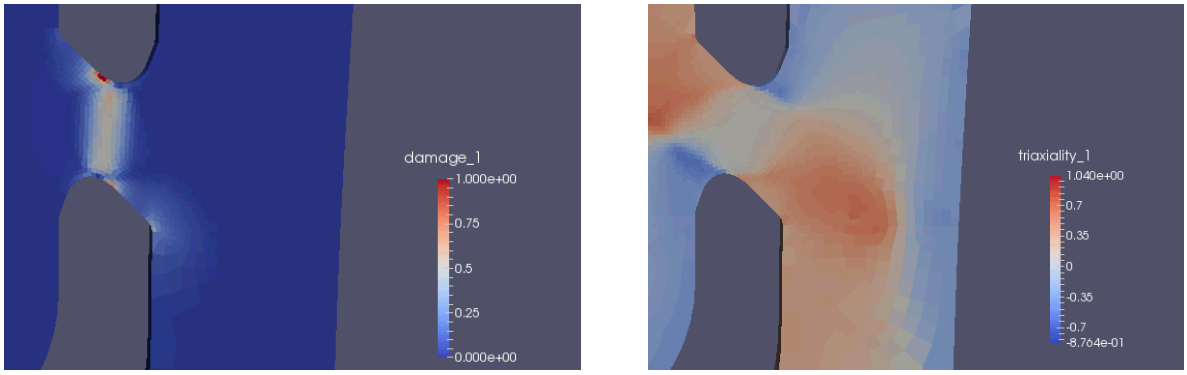

(a) (b)

Figure 18: Results of analysis for the smiley specimen and Al 7075. (a) Contours of Johnson-Cook damage and (b) contours of stress triaxiality.

DISCUSSION:

The objective of the project was to identify test specimen geometries that can be used to test the ductile failure of metals when subjected to states of stress that are shear-dominated and therefore provide data needed in the model calibration process. A combined analytical and experimental process was conducted to achieve the objective. Although careful analyses of the data obtained

in the tests and of the calibration process still need to be conducted, the initial results provided enough information for a first assessment.

Two of the test geometries seem promising, at least for materials that are moderately ductile such as aluminum alloys: the hat and the butterfly specimens. The hat specimen is easily tested in compression, thus requiring just a standard uniaxial load frame with platens. An important geometric feature that makes this specimen work is that all the fillet radii on the edge of the high shear zone have their radius of curvature decrease with deformation, thus keeping the triaxiality over the edges of the regions of interest near zero, as shown in Fig. 6(b). This is a result of the combination of compressive loading and the quarter-circle geometry of the fillets. By contrast, the root of the notches of the EDM-notch and the smiley specimen were in essence half circles, and in both cases one half of the notches had increases in their radius of curvature, thus increasing triaxiality, which may locally precipitate tensile dominated failure. Depending on the application, the hat geometry may, however, display some disadvantages. For example, the specimens need to be relatively thick in order to prevent buckling under compression. Loading a thin hat specimen in tension does not work either since it would induce tensile-dominated loading at the fillets.

The butterfly specimen shows good promise as a geometry where failure can be attained with low triaxiality, especially if further design optimization can increase the separation between the areas of high damage and of high triaxialty. Interestingly, both the Al 7075 and steel A286 specimens failed rather suddenly in this geometry. Determining where failure originated, however, was beyond the capabilities of the instrumentation used in this study. Future use of high speed video is a possibility to attempt to determine the location where failure originated. Whereas the use of the butterfly geometry required the use of a testing device that could apply direct shear to beam-like specimens, more widespread use of this geometry could be achieved if it could be adapted to testing using standard uniaxial test frames. A possible specimen geometry adapted to tensile loading is shown in Fig. 19. The specimen could be gripped using standard hydraulic grips to prevent rotation, thus inducing a similar state of stress in the test section as that obtained with the direct shear apparatus used in this study.

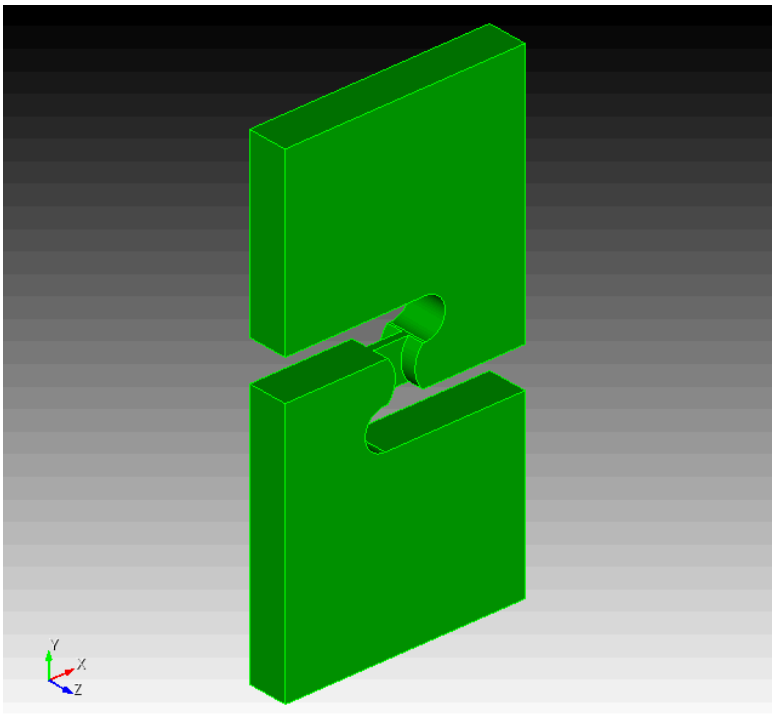

Figure 19: Possible butterfly geometry that can be tested in a tensile test frame.

All the analytical work in this study used the Johnson-Cook failure model to determine when material failure would occur. Clearly, assuming a failure model biases the results, especially during specimen design. Therefore, it is important to always keep this fact in mind and approach the test results with an open mind. It is not until after examining the results carefully that conclusions can be drawn regarding material failure. Based on the results obtained for the hat specimen, the Johnson-Cook failure model fitted the combined failure data from this and other projects well for Al 7075. In other words, a fit determined in [6] based on high triaxiality stresses induced via tension of notched specimens was found to also be valid in the low triaxiality regime. The same, however, was not true for steel A286. The fit obtained using tension of notched specimens did not agree with the results obtained from the hat specimen. Although somewhat disappointing, this result was not unexpected. Given that the failure models are phenomenological, their range of applicability can be constrained by the choice of material and the states of stress being considered.

Whereas significant progress was made during the duration of the project, much work remains ahead to fully analyze the results obtained and ensure that all failure results obtained are consistent with each other. This means, for example, verifying that the Johnson-Cook model's results are consistent across all the Al 7075 specimens tested in this project. Along the same lines, although at the present a failure model for the steel A236 specimens that extends into the low triaxiality has not been identified, it would still be possible to assess if the results are consistent across the tests considered here and in other projects. Finally, identifying a failure criterion that fits the steel failure data would be a significant advance.

Built on
LDRD
Laboratory Directed Research and Development

ANTICIPATED IMPACT:

The research conduced in this project began to address an important aspect of ductile failure that has hitherto received limited attention at Sandia: the acquisition of test data for failure under shear-dominated states of stress. The availability of this kind of information makes it possible to either calibrate or at least test the calibration of material models used in the simulation of structural response and failure under severe mechanical environments. It is therefore important to make shear testing of materials more accessible via standardized test configurations thereby bringing it into the mainstream. Only when this is accomplished will analysts feel that including data from these tests is a practical option that they have available to gain further confidence on their analysis' predictions. Although work remains to be done to carefully analyze the results obtained here, one may conclude that at least two of the four test specimen geometries considered are promising as practical options for routine shear testing.

The immediate next steps to keep moving the topic of ductile failure forward include: completing the analysis of the test and simulation data that resulted from the current project and extending the work on ductile failure into the high strain rate regime.

Carefully reviewing the data generated in this project is an important step to firmly establish the impact of the results that have been obtained so far. One of the most important activities is to compare the test results to the analysis predictions for Al 7075 and to compare the results obtained via the various tests for both materials to establish failure trends with respect to the state of stress.

A great proportion of problems of interest to Sandia involve impulsively applied loads such as those generated by impact or blast. In many cases the strain rates that the material experiences can be high, in the order of hundred or thousands per second. It is therefore important to explore the ductile failure of materials at such strain rates. As in the quasi-static case, it is important to also see how the deformation at failure depends on the state of stress. Therefore, in a complete study not only should we vary the strain rate, but also the state of stress. The results obtained from the data generated in the current project are important to help choose appropriate specimen designs that can be used to investigate shear-dominated failure at high strain rates. It seems, for example, that the hat geometry could be adapted for testing in a split Hopkinson bar compression apparatus for testing at high strain rate.

Two funding streams are currently being pursued to accomplish these immediate next steps. The first consists of WSEAT funding for the development of experimental techniques that will be needed to conduct the investigation of ductile failure at several states of stress over several decades of strain rates, including intermediate ones. The work planned will also include two materials, one with low and another with high values of strain to failure. The second funding stream sought is an exploratory LDRD for FY17 to first carefully analyze the results obtained in

FY16 and then evaluate ductile failure model forms that may be applicable for dynamic strain rates. Preliminary assessment of the models will be based on new dynamic data to be collected under the WSEAT project mentioned previously.

The impact of expanding our experience with ductile failure modeling through research and development efforts has several components. First, it will help identify what the actual failure material behavior is for materials under various states of stress and strain rates. This will allow analysts to choose appropriate material failure models for simulations of actual structural problems of interest, which is the second component. Third, it is important that a standard suite of tests be developed to simplify both the testing efforts and to demonstrate to analysts that the material data that they need can be practically obtained in the laboratory in a reasonable period of time. In the end, the potential main impact of this work lies on improving the credibility of the numerical simulations involving ductile failure that Sandia's analysts conduct. This, in turn, will allow for better decisions to be made regarding the design of Sandia's products, better estimates of the response of these products under severe environments resulting in, for example, more robust qualification processes and a more relevant participation by Sandia in the national security stage.

CONCLUSION:

This project focused on the search for specimens that could be used to provide information about ductile failure when the material is subjected to shear-dominated states of stress. This data can then be used to either estimate the performance of material failure models when the stress triaxiality is low or to calibrate them. Two materials were considered: aluminum 7075 and steel A286 to explore the dependence of the results on the material. From our point of view, the main difference between the two alloys was their ductility; the aluminum alloy's being significantly less that that of the steel. The work was carried out using a combination of analysis and experimentation. Although all the specimen design, testing and preliminary analysis were completed, more in depth analysis of both the test data and the analysis results need to be conducted in the future to draw better grounded conclusions.

Out of the four test specimen geometries considered (hat, EDM-notch, butterfly and smiley) the hat and the butterfly specimens showed good promise as candidates to provide the desired data, at least for the aluminum alloy. The criterion to determine whether a particular geometry could yield the desired data had two steps: (1) Using the Johnson-Cook failure model in the analysis, the point in the specimen where failure was predicted to initiate had to lie in a region where the calculated stress triaxiality was near zero, as this value indicates a shear-dominated state of stress. (2) From observations in the experiments, the measured load and deflection of the specimen at failure was obtained and compared to the analysis predictions to see if they were close. Although it was not always possible to determine the exact location where failure initiated in the specimens, at least one could check whether the fracture passed through the region where the analysis predicted failure initiation.

Of course, having chosen the Johnson-Cook failure model biases our results and therefore the step involving the comparison between the analysis and tests results are compared is crucial. In this work, the results for the aluminum alloy obtained with the hat specimen correlated well with the predictions of the Johnson-Cook model, but the results from the other geometries still need to be analyzed. The results for the steel alloy, on the other hand, did not follow the predictions of the Johnson-Cook model.

Besides reviewing the results of this study more carefully to make our conclusions firmer and investigate what failure model could be used to computationally reproduce the results of the steel specimen, the next step should include extending our work on ductile failure to the high strain rate regime, especially given that many of the applications of interest at Sandia involve dynamic loading. Projects to address dynamic loading are being planned, both from the testing point of view to develop the instrumentation and experimental techniques that will be needed, as well as from the analysis point of view to identify candidate models that could be used in this regime.

REFERENCES

[1] Johnson G.R. and Cook W.H., "Fracture characteristics of three metals subjected to various strains, strain rates, temperatures and pressures," *Engineering Fracture Mechanics*, V. 21, pp. 31-48, 1985.

[2] Corona, E., Deibler, L.A., Reedlunn, B., Ingraham, M.D. and Williams, S., An experimental study of shear-dominated failure in the 2013 Sandia Fracture Challenge specimen, Sandia Technical Report SAND2015-2850, 2015.

[3] Kramer, S.L.B., Characterization of 304L stainless steel laser welds, Sandia Technical Report SAND2015-9012, 2015.

[4] Dunand, M. and Mohr, D., On the predictive capabilities of the shear modified Gurson and the modified Mohr-Coulomb fracture models over a wide range of stress triaxialities and Lode angles, *Journal of the Mechanics and Physics of Solids*, V. 59, pp. 1374-1394, 2011.

[5] Roth, C.C. and Mohr, D., "Ductile fracture experiments with locally proportional loading histories," *International Journal of Plasticity*, V. 79, pp. 328-354, 2016.

[6] Corona, E. and Orient, G.E., An evaluation of the Johnson-Cook model to simulate puncture of 7075 aluminum plates, Sandia Technical Report SAND2014-1550.